# Illite-smectite patterns in sheared Pleistocene mudstones of the Southern Apennines and their implications regarding the process of illitization: A multiscale analysis

Emilio Casciello [a,*], John W. Cosgrove [b], Massimo Cesarano [c], Enrique Romero [d], Ignasi Queralt [a], Jaume Vergés [a]

[a] Group of Dynamics of the Lithosphere (GDL), Institute of Earth Sciences "Jaume Almera", CSIC, Lluís Solé i Sabarís s/n, 08028 Barcelona, Spain
[b] Department of Earth Science and Engineering, Royal School of Mines, Imperial College, Prince Consort Road, London SW7 2BP, UK
[c] Department of Science and Technology for the Environment and Territory, University of Molise, C.da Fonte Lappone, 86090 Pesche (IS), Italy
[d] Department of Geotechnical Engineering and Geosciences, Universitat Politècnica de Catalunya, c/Jordi Girona, 1-3 Campus Nord UPC, Barcelona, Spain

## ARTICLE INFO

## ABSTRACT

The transformation of water-rich smectite clay minerals into relatively anhydrous illite is a common reaction in sedimentary basins. It is commonly thought to be driven by temperature increase with increasing burial depth. This mineral transformation is also observed in the gouge of large faults, and because it releases bound water from smectite, it is thought to be a key control in hydrologic and mechanical processes at subduction complexes. In this work, the distribution of smectite and illite within a large fault zone of the Southern Apennines of Italy is analysed at scales varying from outcrop to sub millimetre. X-ray diffraction analyses indicate a direct link between the darkening in colour of the sheared mudstone and the illitization of smectite. The heterogeneous distribution of illite and smectite within this shear zone was studied by integrating outcrop-scale observations with a peeling technique that allows microscope and SEM observations to be made over areas in excess of 60 cm$^2$. The observed patterns of smectite illitization suggest that temperature is not the primary cause of the mineral transformation inside the fault. The distribution of illite along planes of the P foliation and in the infill of shears indicates that shear stress facilitates the mineral transformation.

© 2011 Elsevier Ltd. All rights reserved.

## 1. Introduction

The behaviour of mudstones subjected to shear deformation and the properties of the resulting shear zones have been analyzed by many researchers yielding a vast literature (e.g. Maltman, 1987; Vrolijk and van der Pluijm, 1999; Solum and van der Pluijm, 2009; Ikari et al., 2009). Fluid-flow and frictional properties, mineralogical composition and stress state are all interacting aspects of a complex phenomenon, the shearing of clay-rich materials, that concerns fields of research as varied as hydrocarbon exploration, waste containment, seismology, geochronology and plate tectonics. In hydrocarbon systems, mudstones generally correspond to source rocks and/or seals. Therefore, the fluid-flow

properties of faulted seals are clearly a crucial issue when assessing their integrity with respect to oil or CO$_2$ traps (Ingram and Urai, 1999; Dewhurst and Hennig, 2003; Bailey et al., 2006). In addition, the diagenetic evolution of clay-rich sediments and the transformation of smectite to illite is linked to the migration and trapping of hydrocarbons (Weaver, 1960; Bruce, 1984; Zeng and Yu, 2006; Abid and Hesse, 2007). The transformation of water-rich smectite into the relatively anhydrous illite has also been invoked to explain salinity anomalies encountered during the Ocean Drilling Program (ODP) and Deep Sea Drilling Project (DSDP) on the Nankai and the Barbados accretionary wedges. In both wedges, high pore pressure and pore water freshening are recorded across the main décollements (e.g. Bangs et al., 1999; Brown et al., 2001; Maltman and Vannucchi, 2004), sparking debate over the source of this fresh water, the distances these fluids can travel, the possibility of overpressure build-up and consequently, also on seismicity and stress state at plate boundaries (e.g. Shipley et al., 1994; Saffer and Bekins, 1998, 2006; Fitts and Brown, 1999; Brown et al., 2001, 2003; Moore and Saffer, 2001; Faulkner and Rutter, 2001; Saffer and

Marone, 2003; Henry and Bourlange, 2004; Ujiie et al., 2009; Tobin and Saffer, 2009).

The evolution of a shear fabric in phyllosilicate-rich materials and its effects on permeability and frictional properties have been analyzed mainly through laboratory experiments using natural or synthetic materials (e.g. Maltman, 1987; Moore et al., 1989; Arch and Maltman, 1990; Logan et al., 1992; Dewhurst et al., 1996; Zhang and Cox, 2000; Bos and Spiers, 2001; Takizawa et al., 2005; Ikari et al., 2009). However, comparatively few studies have focused on exposed shear zones in clay-rich deposits, and even fewer report on the smectite to illite transformation within exposed faults (Vrolijk and van der Pluijm, 1999; Casciello et al., 2004; Solum et al., 2005; Dellisanti et al., 2008; Haines et al., 2009). In this contribution, the detailed features of a shear zone deforming early Pleistocene mudstones of the Sant'Arcangelo Basin, in southern Italy (Fig. 1), are examined. Earlier work on this fault showed that both footwall and hangingwall contain mixed-layer illite/smectite while the sheared mudstones contain only illite clay minerals. This mineral distribution indicates that faulting enhanced the transformation of smectite into illite (Casciello et al., 2004). We present a detailed analysis of the distribution of smectite and illite within the shear zone and the results of a consolidation test aimed at defining the depth of formation. The patterns of smectitic and illitic mudstone were studied using a peeling technique that permits

analysis the shear fabric and the compositional heterogeneities using a petrographic microscope and scanning electron microscope (SEM). This approach provides considerable insight into the smectite to illite transformation inside a large natural fault, at a wide range of observational scales.

## 2. Geological setting of the shear zone

The shear zone analyzed in this paper is a segment of a regional scale discontinuity, known as the Scorciabuoi fault, which traverses the easternmost foothills of the Southern Apennines with a WNW-ESE trend and left-lateral displacement (Fig. 1). The Scorciabuoi fault is a high-angle (>70°), south dipping discontinuity that can be traced for approximately 30 km, dissecting allochtonous thrust sheets and their Plio-Pleistocene sedimentary cover (Carbone et al., 1991; Benvenuti et al., 2006). This fault is interpreted as an oblique ramp of the ENE-verging Valsinni blind thrust system, in which the fault terminates (Bonini and Sani, 2000; Hippolyte et al., 1994a; Monaco et al., 1998, 2001). The growth of the Valsinni ridge in Early-Mid Pleistocene times separated a vast area of the Pliocene marginal foredeep from the main foredeep. Within this marginal foredeep area, now known as the Sant'Arcangelo Basin, a gradual switch from marine to continental deposition occurred (Pieri et al., 1994; Benvenuti et al., 2006). The age of activation of the
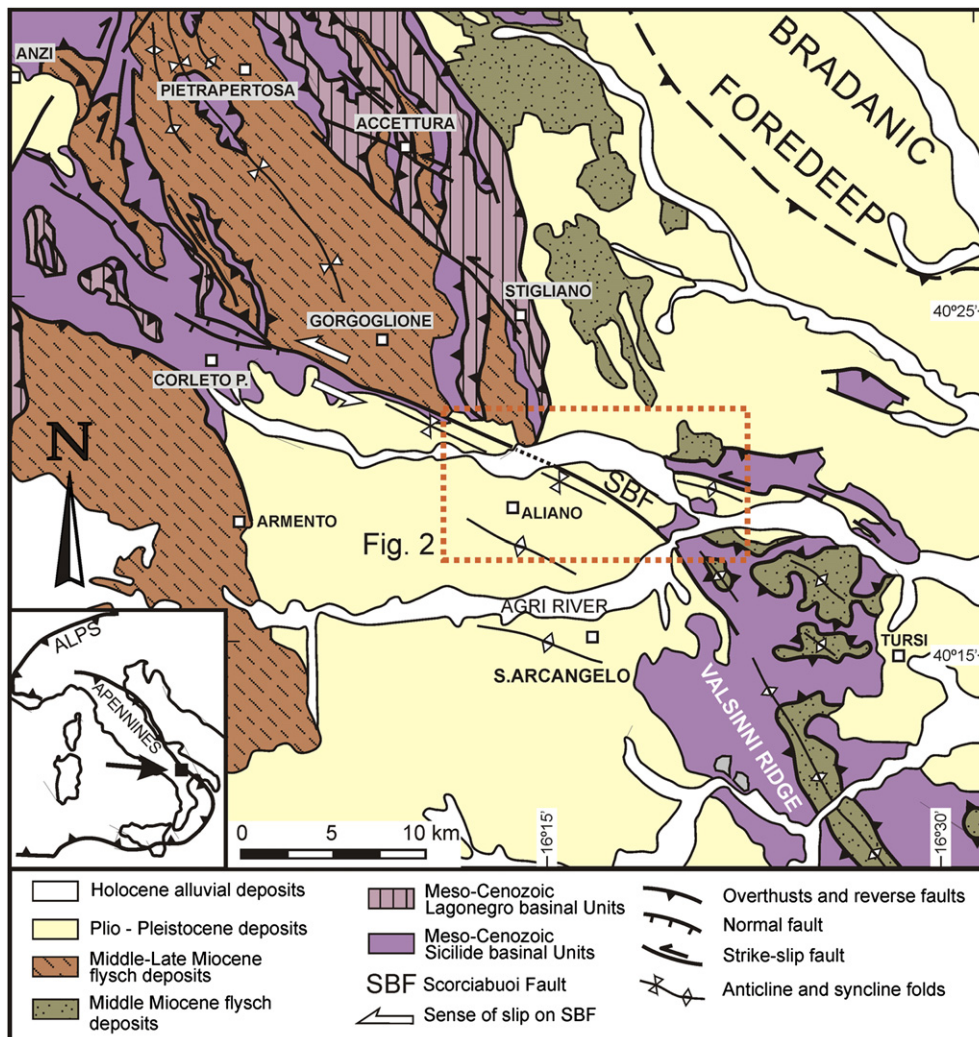


**Fig. 1.** Geological map of the northern part of the Plio-Pleistocene Sant'Arcangelo basin (after Casciello et al., 2004).

Scorciabuoi fault is therefore linked to the uplift of the Valsinni ridge and is generally defined as Early to Mid Pleistocene (Bonini and Sani, 2000; Catalano et al., 2004; Benvenuti et al., 2006). Nevertheless, recent morphotectonic studies provide evidence that demonstrates that fault activity continued throughout the Late Pleistocene and Holocene, indicating that the Scorciabuoi fault is a still active and potentially seismogenic structure (Caputo et al., 2008). Existing earthquake catalogues (http://csi.rm.ingv.it/), however, do not support conclusively the seismogenic activity hypothesised by Caputo et al. (2008). Kinematically, the fault possibly changed from sinistral transtension to normal dip-slip between 0.7 and 0.5 Ma (Pieri et al., 1997) or slightly later (Caputo et al., 2008). This interpretation is in agreement with a generalized change of the stress regime from WSW-ENE compression to NE-SW extension that is recorded throughout the Southern Apennines (Hippolyte et al., 1994b; Maggi et al., 2008). However, the field evidence for such a kinematic transition along the Scorciabuoi fault is unclear because preserved structures observed along the fault relate uniquely to sinistral slip movement.

The sheared mudstones analyzed in this study form part of a thick and rather homogeneous marine succession of silty-marly mudstones that comprise both the Pliocene deposits of the marginal foredeep stage (Cd deposits in Benvenuti et al., 2006) and the overlying early Pleistocene mudstones of the Sant'Arcangelo Basin fill (Ad deposits in Benvenuti et al., 2006). These predominantly clayey deposits are widely exposed in the eastern part of the Sant'Arcangelo basin, and in the area between the Sauro stream and the Agri River (Fig. 1) they are deformed by the Scorciabuoi fault. Because of the transtensional displacement along this fault, the footwall (northern block) exposes Pliocene mudstones while the hangingwall (southern block) is composed of the Early Pleistocene part of the succession, which is composed by about 1000 m of marly mudstones with overlying partially heteropic sandstones and conglomerates (Fig. 2; Benvenuti et al., 2006). The bedding in both the footwall and the hangingwall dips about 20° to the north on average and the rocks lacked significant deformation prior to the fault formation.

## 3. Outcrop scale analysis

Various outcrops of sheared mudstones occur along the analysed segment of the Scorciabuoi fault; however, we focused on one complete exposure of the shear zone with ease of access and continuity of exposure (site A in Figs. 2 and 3; Google-Earth placemark in supplementary material). In this outcrop, the sheared mudstones characteristically have a darker colouring with respect to the surrounding undeformed material, and comprise a 5 m wide belt of intensely deformed material (Fig. 3). The margins separating the undeformed wallrock from the darker, deformed mudstone of the shear zone are very sharp. Lenses or streaks of relatively undeformed material, discerned by a lighter colour, are enclosed within the shear zone and their long axes are parallel or moderately oblique to the shear zone boundaries. The dimensions of such embedded lenses vary from centimetres to several metres (Fig. 4). Topographically, the dark portions have a greater relief in exposure than the light coloured mudstones forming the wallrock and lenses within the shear zone. Both sheared mudstones and the light-coloured lenses display a pervasive foliation highlighted by the preferred orientation of desiccation cracks, which form angles of 135°−180° with the shear zone boundary (Fig. 5). This foliation, known as a P foliation (Fig. 6A), is characteristic of clay-rich fault gouges and experimentally produced shear zones (Rutter et al., 1986; Dewhurst et al., 1996; Bos and Spiers, 2001; Haines et al., 2009), reflecting the intense strain-induced preferred orientation of clay platelets. The P foliation is transected by differently oriented sets of minor shear surfaces. Based on the angle that these various shear sets form with the shear zone boundary we group them as $R_1$-shears, P-shears and Y-shears (Logan et al., 1992; Fig. 6B).

The character of the dark bands of the shear zone is more clearly exposed where the Sauro stream crosses the shear zone (site B, Fig. 2). Here the stream has removed the weathered superficial layer allowing direct observation of the structural geometries within the zone. A recurrent geometry found in this outcrop is shown in Fig. 7. On the inner side (i.e. opposite to the direction of tectonic transport) of light-coloured lenses embedded in the shear
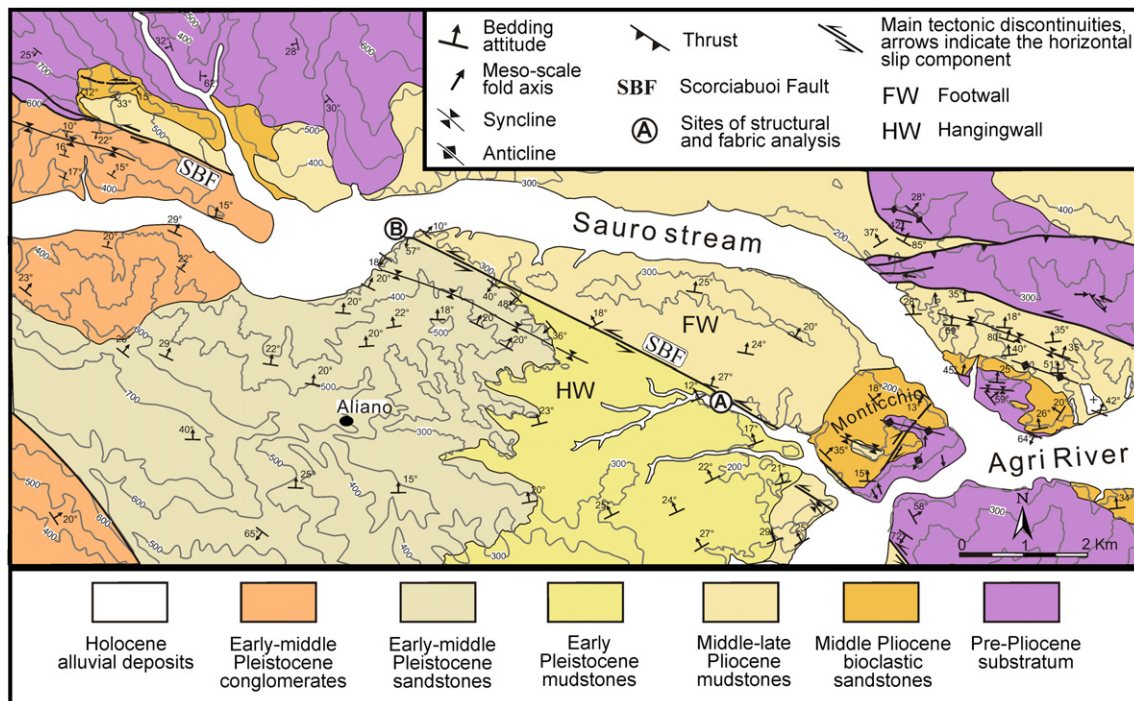


**Fig. 2.** Geological map of the area around sample sites along the Scorciabuoi fault. Location in Fig. 1.

**Fig. 3.** Field picture of the analyzed shear zone. Its location is A in Fig. 2 and is also indicated by a Google-Earth placemark in the supplementary material. The shear zone appears as a 5 m wide belt of dark mudstones enclosing lenses and streaks of relatively undeformed material, discerned by a lighter colour. (For interpretation of the references to colour in this figure legend, the reader is referred to the web version of this article.)

zone, P and Y-shears combine to create geometries similar to thrust or strike-slip duplexes (Boyer and Elliot, 1982; Woodcock and Fischer, 1986). The horses of these duplexes are shear lenses elongated in the direction parallel to P-shears, while the roof and sole thrusts are formed by Y-shears or bands of anastomosed Y-shears. By analogy with duplex systems of thrust systems, this geometry is interpreted to form through the progressive collapse of the lighter coloured mudstone of the host rock into the strike-slip duplex, leading to the 'erosion' (i.e., the decrease in size) of the undeformed domains with increasing shear strain.

### 3.1. X-ray diffraction analysis

Samples of the footwall, of the hangingwall and of the dark, sheared mudstone from the studied outcrop (Figs. 3 and 4) were analyzed by X-ray diffraction (XRD) to characterize the clay mineral content and to confirm previous analyses indicating complete smectite disappearance from the dark sheared clays (Casciello et al., 2004). Analyses were performed at the Laboratory of X-ray and Analytical Applications (LARX) of the Institute of Earth Sciences 'Jaume Almera' − CSIC, Spain, using a Bruker D-5005 diffractometer, with Cu radiation and secondary Graphite monochromator. The range of $2\theta$ was of $4°-60°$ and $2°-40°$ for the powder samples and oriented aggregates respectively. Both air dried and ethylene glycol solvated samples were analysed.

Whole-rock analyses show a very similar composition for the footwall and the hangingwall, with quartz, calcite and Na-feldspars forming the non-clay fraction and smectite, illite, chlorite and kaolinite as the clay minerals (Fig. 8). Semi-quantitative analysis indicates the clay fraction represents 40−50% of both samples. The presence of expansible smectites in the footwall and in the hangingwall is highlighted by the appearance of a peak around $5°$ $(2\theta)$ in the ethylene glycol solvated samples, corresponding to the maximum hydration state of smectite with a basal spacing of approximately 18 Å (Colten-Bradley, 1987). An estimate of the hydration state of the smectites in the footwall and hangingwall was obtained from the profiles of dry aggregates in the interval between $6°$ and $9°$ $(2\theta)$. In both profiles, the average basal spacing in the smectites of the mixed layer illite/smectite is around 11 Å, which corresponds to the presence of only 1 layer of water between alluminosilicate sheets (Colten-Bradley, 1987). By contrast, the ethylene glycol solvated diffraction profile of the dark mudstones within the shear zone indicates that no smectite is present. This result confirms previous analyses for 6 samples extracted from different sites along the Scorciabuoi shear zone (Casciello et al., 2004) and strengthens the evidence for greater illite content in mixed layer illite/smectite sediments involved in faulting (Vrolijk and van der Pluijm, 1999; Solum et al., 2005; Haines et al., 2009).

The peak-full-width at half maximum (FWHM) values, a function of crystallite size and/or structural order (Merriman and
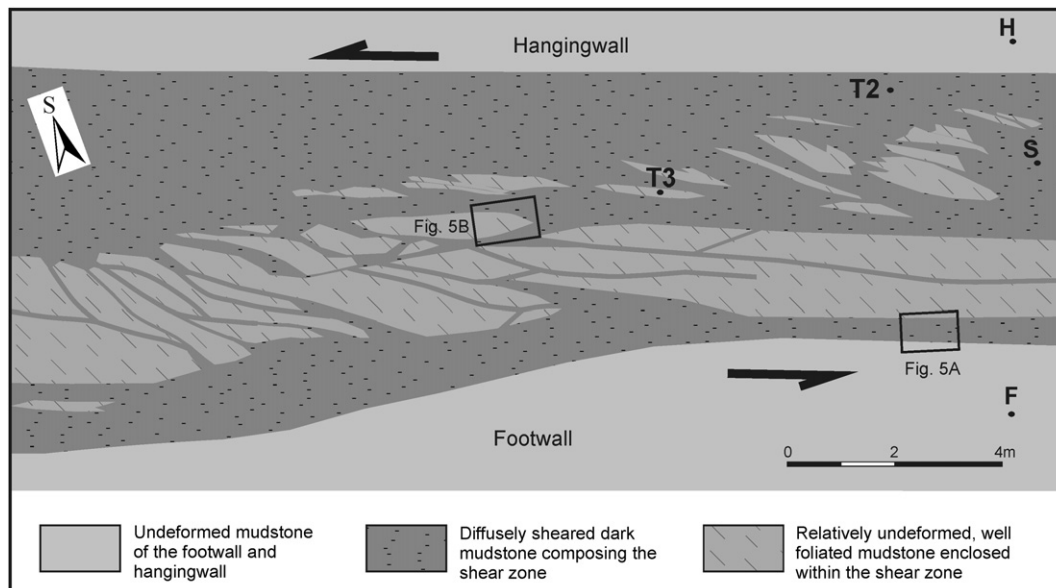


**Fig. 4.** Sketch of the exposure with location of the large samples used to obtain peels (T2, T3), of the samples used for X-Ray diffraction (F, S, H) and for Fig. 5.
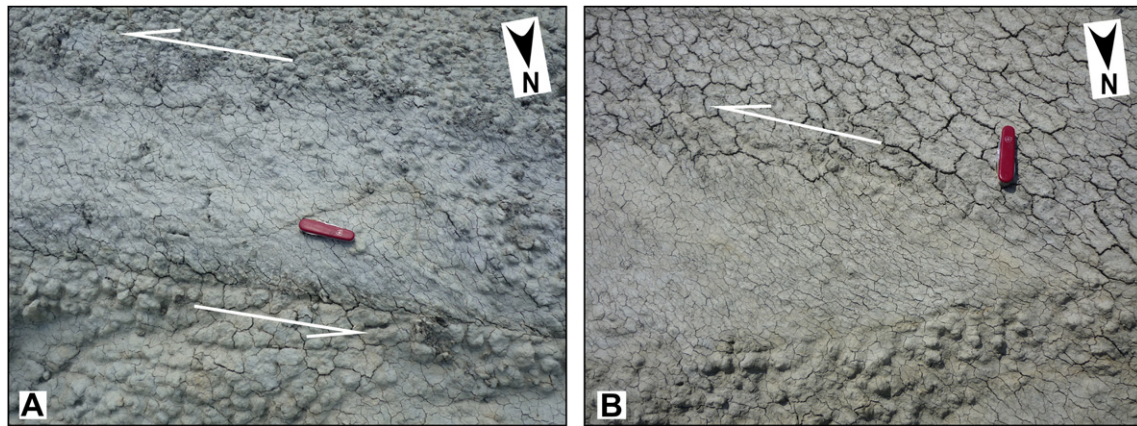
**Fig. 5.** Tectonic foliation within the shear zone is highlighted by the preferred orientation of desiccation cracks. A) The aligned cracks of the shear zone form an angle of 144° with the northern margin at which they terminate. Knife is 9 cm long. B) Example of embedded lens of relatively undeformed material within the shear zone. The lens is affected by iso-oriented desiccation cracks displaying a slightly curving trajectory and terminate at 165°, at lens boundary in shear zone.

Peacor, 1999), for the 001 illite peak ($\sim 10$ Å/1 nm) show averages of 0.46° in the undeformed wallrock and 0.28° for samples inside the shear zone, indicating a greater 'crystallinity' of the sheared material, and supporting the idea that fault-related changes in mineralogy have occurred (e.g., Vrolijk and van der Pluijm, 1999; Yan et al., 2001; Solum and van der Pluijm, 2009).

## 4. Sample scale analysis

In addition to samples collected for XRD analysis, other oriented samples, up to 20 cm in size, were collected from within the shear zone and from the light-coloured lenses enclosed within it (Fig. 4) to study the micro-structures of the shear bands. Since the mudstones of the Sant'Arcangelo basin are indurated, samples were chiseled out of the shear zone. On these large samples a peeling technique similar to that employed to analyse sedimentary features in carbonate rocks (e.g. Brown, 1986) was tested with positive results (Casciello et al., 2004). Peels created with this technique are sufficiently transparent to be observed with a standard optical microscope and to be imaged using a retro-illuminated scanner. In addition, peels can be samples for SEM analysis, integrating centimetre-scale observations directly with micron-scale observation. High-resolution scan images of the peels are available as supplemental material.

### 4.1. Sample preparation for peeling

Fresh samples (i.e. samples not affected by surficial weathering) were cut along a plane perpendicular to the tectonic foliation (P foliation in Fig. 6A) and containing the shear direction, using an ordinary circular saw with no lubricating fluid. Fragile samples were encapsulated in polyurethane foam prior to cutting. To eliminate scratches and grooves from the cut plane and to obtain a perfectly planar surface, the cut plane was smoothed using carborundum abrasive disks on a lapping machine, again without lubricating fluid. For the initial smoothing, a grain size of 180 (125 μ) was used, while a finer grain size of 1000–1200 (18–14 μ) was employed to finish the surface. The planes of observation were then cleaned and covered with a thin (<1 mm) layer of Araldite resin (LY 554) prepared at room temperature by mixing it with a catalyst (HY 956) in a proportion of 5-1 parts by weight. Samples dried in an oven at 50 °C and atmospheric pressure for 24 h, keeping the surface with the resin perfectly horizontal. Removal of the Araldite resin film from the surface of the sample after drying yields the peel of the sample, which is a thin layer of material fastened to the resin, preserving the fabric and the compositional heterogeneities of the sample. The amount of material adhering to the resin depends on the porosity and mechanical properties of the sample. In the same way that the weaker, light bands of smectitic
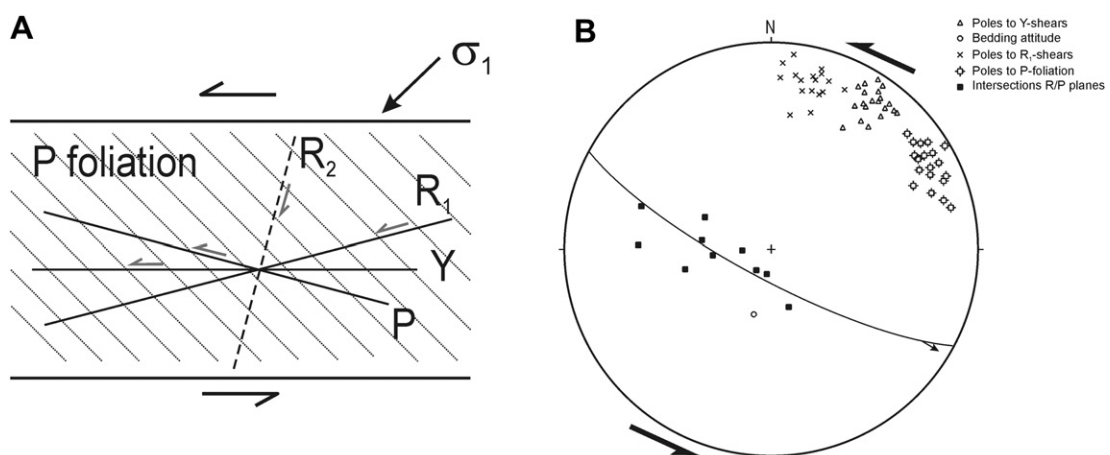


**Fig. 6.** A - Terminology of shear-related features for this work (after Logan et al., 1992). B — Equal-angle, stereographic projection for orientations of fabric features in studied exposure (after Casciello et al., 2004).
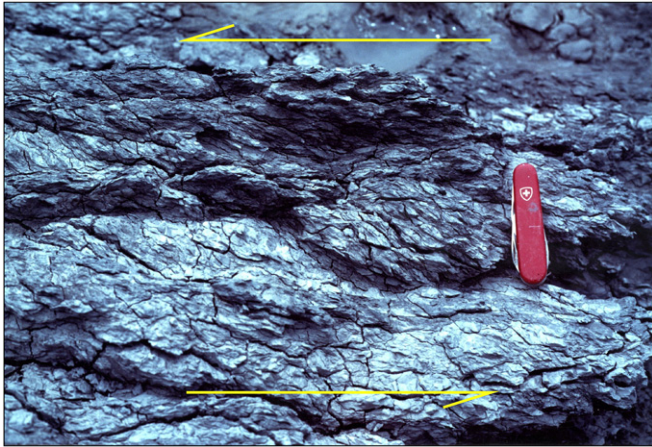
**Fig. 7.** Detail of the shear zone in location B of Fig. 2. Fabric elements combine to create a strike-slip duplex geometry in which the footwall is composed of the relatively undeformed, lighter coloured mudstone, while the roof thrust and the duplex horses are formed by intensely sheared and darker mudstone. Differential erosion causes the darker parts to stand out with respect to the light coloured less-strained mudstone.

clay erode more easily than the illitic dark bands to produce outcrop relief (Fig. 7), so the light-coloured smectitic portions of the samples are more easily bound by the Araldite resin and leave a larger quantity of mudstone on the peel, whereas the more cohesive darker parts (illitic) leave only a thin film of material (Fig. 9). Therefore, when the peel is observed in transmitted light, the thicker quantity of clay left on the peel for the smectitic parts

produces darker areas, while the thinner quantity for the dark illitic mudstone generates brighter areas (Fig. 10).

### 4.2. Sample T2

This sample was extracted from the southern margin of the shear zone (Fig. 4), from a wide and macroscopically uniform band of dark sheared mudstone. The peel (Fig. 10) displays darker domains contained in a light coloured 'matrix'. As discussed, these dark portions of the peel correspond to the light coloured mudstones that form the wallrock of the shear zone and the lenses embedded within it, while the light coloured 'matrix' corresponds to the dark sheared mudstone (Fig. 9).

To confirm that the darkening of the mudstones corresponds to the replacement of smectite by illite, XRD analyses where conducted on dark and light areas of this sample (Fig. 10). The results confirm that even at the subcentimetre scale the darker clays (i.e. lighter areas in Fig. 10) correspond to domains of illitization and smectite disappearance (Fig. 8). This finding demonstrates that the peels are detailed reproductions for the patterns of smectite illitization within the shear zone.

Approximately 61% of the total area (62.3 cm$^2$) of peel T2 is formed by illitic mudstone, the remaining part contains mixed layer illite/smectite (smectitic mudstone hereafter). This latter component forms a few larger belts, several centimetres long and approximately one centimetre-wide elongated parallel or at a small angle to the shear direction and numerous smaller bandings elongated parallel to the P foliation with millimetre to sub-millimetre spacing (Fig. 11). When observed with a universal-stage microscope, the contrast between the illitic and smectitic
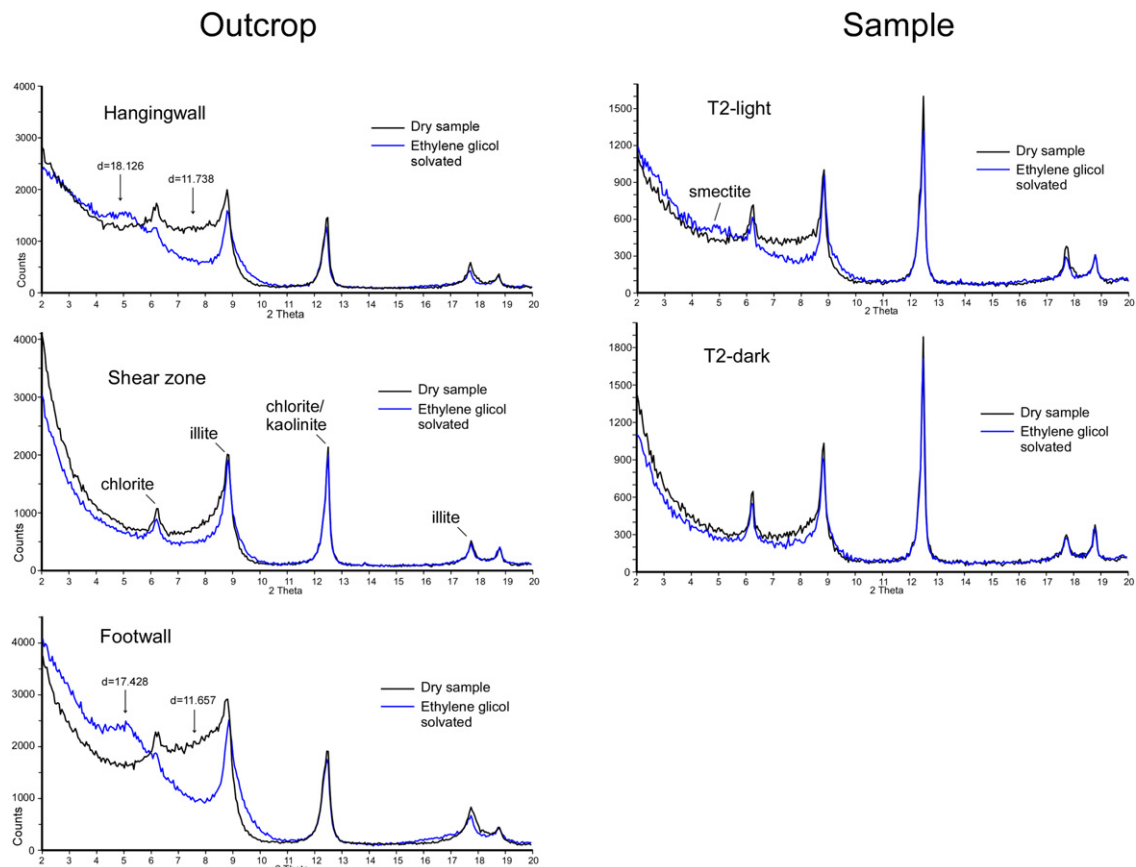


**Fig. 8.** X-ray diffraction analyses of samples extracted from the exposure pictured in Fig. 3 (left) and on material extracted from the sample T2 (right). In both cases, the dark-coloured sheared mudstone lacks smectite minerals.
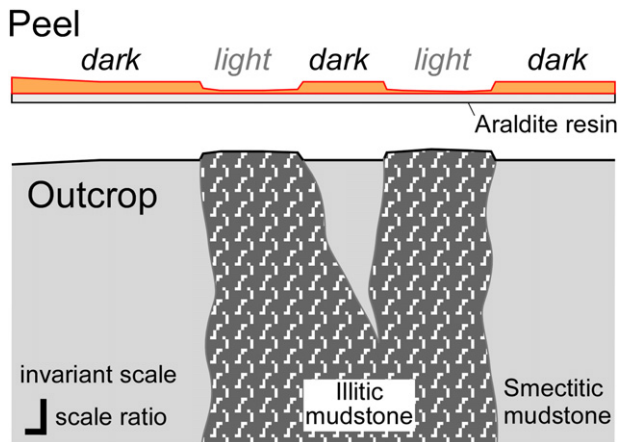
**Fig. 9.** Sketch illustrating the reversal in colour between the outcrop and the peels when these latter are observed in transmitted light. The topographic effect caused by the illitic gouge, and the selective fastening of the Araldite resin are also represented. (For interpretation of the references to colour in this figure legend, the reader is referred to the web version of this article.)

mudstone is amplified because of the greater thickness of smectitic mudstone adhering to the peel, as mentioned in Section 4.1. Illitic parts appear finer grained than the smectite-rich component and under crossed Nicols they display bluish interference colours (Fig. 11B). Observation with crossed Nicols facilitates the recognition of microshears within the illitic component that are otherwise not visible (e.g., Fig. 11D vs. 11C). On a larger scale, shears are not detectable within the illitic component (Fig. 10), so they can only be recognized where the smectitic mudstone is juxtaposed against the illitic.

### 4.3. Sample T3

Sample T3 was taken from a small lens of light-coloured mudstone embedded in the central part of the shear zone (Fig. 4). In this peel, the proportion of smectitic mudstone (dark on the peel) is much greater than in Sample T2 and the illitic component accounts for only 25% of the peel's area (49.4 cm$^2$; Fig. 12).

The most striking features in this peel are shears filled with light-coloured illitic mudstone. One of these shears, in the upper right corner of Fig. 12, displays irregular margins and its light-coloured illitic filling contains darker streaks of smectitic wall-rock. Microscope observation of the small step located along the lower margin of the shear (Fig. 12 and Fig. 13A) shows that the bright illitic fill has a curving geometry around the lower angle of the step. SEM observation of this area (Fig. 13B), indicates that the illitic fill is cut by microshears that gradually curve with the shear boundary. A close-up of the illitic infill of this shear (Fig. 13C) shows a strong fabric marked by the preferred orientation of elongated particles and microshears. The same parallelism of platy particles is present in Fig. 13D, which shows the sharp contact between the wallrock of the shear and the illitic fill. The similarity with Fig. 4A, depicting the shear zone margin at outcrop scale, is striking. Other shears filled with illite traverse the central part of the peel, mostly oriented as P-shears and like the previous example, their filling are interpreted to result from ductile-like behaviour. A common characteristic of these shears is that they contain fragments of darker smectitic mudstone that are interpreted to be entrained and deformed within the light-coloured illitic infill (Fig. 12). In some segments of the larger shears, these smectitic inclusions are arranged as sub parallel trails, indicating that the same shear experienced multiple events of shearing (M, in

Fig. 12). Illitic veinlets are also well imaged in the peel, as light coloured, hairline-width features within the smectitic component (V, in Fig. 12). When observed with polarized light, these micro-structures display the same bluish interference colours as the illitic parts of the peel and therefore, we assume they contain illite. Under crossed Nicols, one sample area appears composed predominantly of smectitic mudstone, in the form of particles elongated parallel to the P foliation, enclosed in a scarce illitic (bluish) 'matrix' (Fig. 14). This structure indicates that the illitic material not only characterizes the filling of relatively large shears (Fig. 12) but also forms pockets apparently unrelated to significant shear displacement.

## 5. X-ray fluorescence mapping

The patterns of illitic and smectitic mudstones were also analyzed in terms of element distribution by X-ray fluorescence mapping (EDXRF). A small portion of sample T2 (1.5 × 2 cm; Fig. 15A) was mapped using a bench-top energy-dispersive X-ray spectrometer (XDV-SD model, Helmut Fischer GmbH, Sindelfingen, Germany) equipped with a programmable XY(Z) stage that linearly scans or maps point-to-point differences in elemental chemistry or spectral sample density. The chemical mapping is based on 150 point analyses (1 analysis per 2 mm$^2$) conducted using a voltage of 30 kV, current of 0.1 mA, spot size of 1 mm, and an acquisition time of 200 s per point. For calibration, Certified Reference Material (CRM) from the National Resources Canada (STSD-1) was used. Statistical test runs for methodological validation reveal that relative standard deviation for the elements of interest are less than 1%, and the accuracy is between 0.005 and 0.014% (calibration data available as supplementary material). Since the illitization process is expected to produce enrichment in K, Al, Fe, Mg and a depletion of Ca, Si, Na and Cl, with respect to the original smectitic mudstone (Capuano, 1993; Drief et al., 2002), the ratios of K/Ca and Fe/Ca where used to map the sample (Fig. 15B–C). Lighter elements, such as Si, Al, Na and Mg, could not be analyzed because their characteristic energies are largely absorbed by air and the resulting counts would be strongly underestimated. The distribution of K, Ca and Fe matches closely the map patterns of light and dark coloured mudstone, corresponding to the smectitic and illitic mudstone, respectively (Fig. 15). These results confirm once again that the darkening of the mudstone coincides with illitization of smectite and document that appreciable ionic transfer occurred in association with the process.
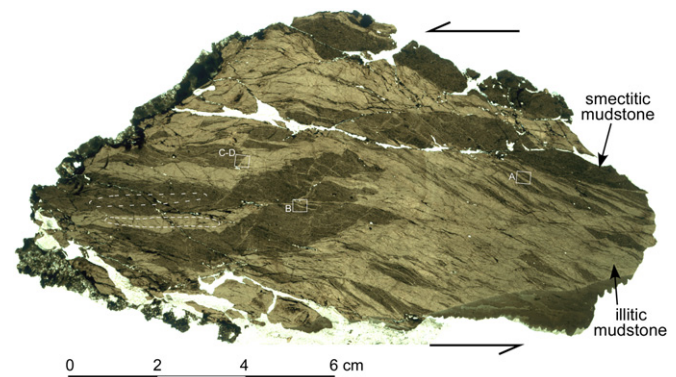


**Fig. 10.** High-resolution scan image of the peel obtained from sample T2, which was extracted from the southern margin of the shear zone (Fig. 4). The plane of shear is horizontal and the sense of shear is sinistral. The white dashed lines indicate areas analyzed by X-ray diffraction (Fig. 8), and the white rectangles locate the microphotographs of Fig. 11. A mark-free image of this peel, with higher resolution, is available as supplemental material.
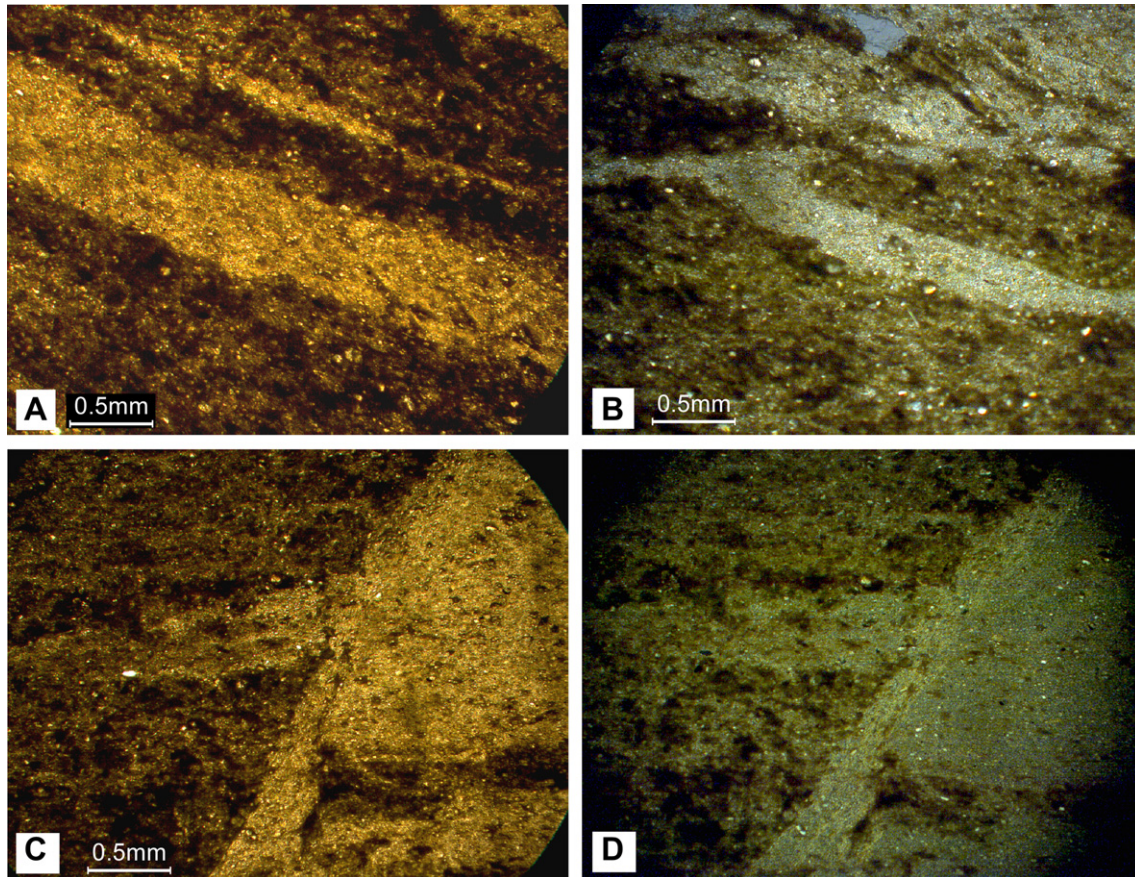
**Fig. 11.** Microphotographs of the peel obtained from sample T2 (Fig. 10). A - Alternating bands of illitic (light) and smectitic (dark) mudstones elongate parallel to the P foliation. The smaller illitic band is only 0.1 mm wide and is enclosed in smectitic mudstone. B - Abutting relationship between illite-filled fractures/shears viewed with crossed Nicols. C - Sharp contact between the smectitic (left) and illitic components in unpolarized light. Crossed Nicols image (D) reveals a belt of light coloured microshears (upper right to lower left) marking the contact on the illitic side and displacing also a faint band of illitic mudstone contained in the smectitic component.

The dark illitic mudstone is enriched in K, Ti, and Fe, while the light coloured smectitic component is relatively enriched in Ca. Enrichment in Ti relative to the smectitic mudstone (2760 mg kg$^{-1}$ and 2170 mg kg$^{-1}$, respectively) is analogous to data reported from the Moab fault (Solum et al., 2005). In that fault, enrichment in Ti with respect to the protholith is attributed to the removal of more mobile elements in association to clay authigenesis.

## 6. Consolidation test

To investigate the burial conditions for the shear zone, a drained oedometer test was conducted on the footwall mudstones. This test to study soil compressibility and consolidation is also used in soil mechanics to determine the overconsolidation ratio (OCR), which is essentially a measure of the uplift (unloading) experienced by
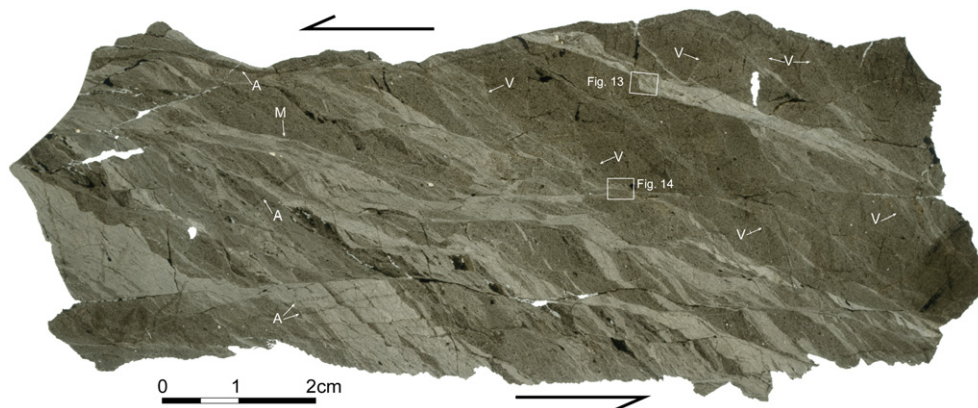


**Fig. 12.** High-resolution scan image of peel from sample T3, which was extracted from a small shear lens in the central part of the analyzed shear zone (Fig. 4). The white rectangles mark the location of Figs. 13 and 14. V, examples of veinlets. M, shear segment with multiple episodes of shearing. A, marks due to peel detachment. N.B. light coloured portions are illitic (i.e., no smectite), dark portions are smectitic (i.e., mixed layer illite-smectite). A mark-free image of this peel is available as supplemental material.
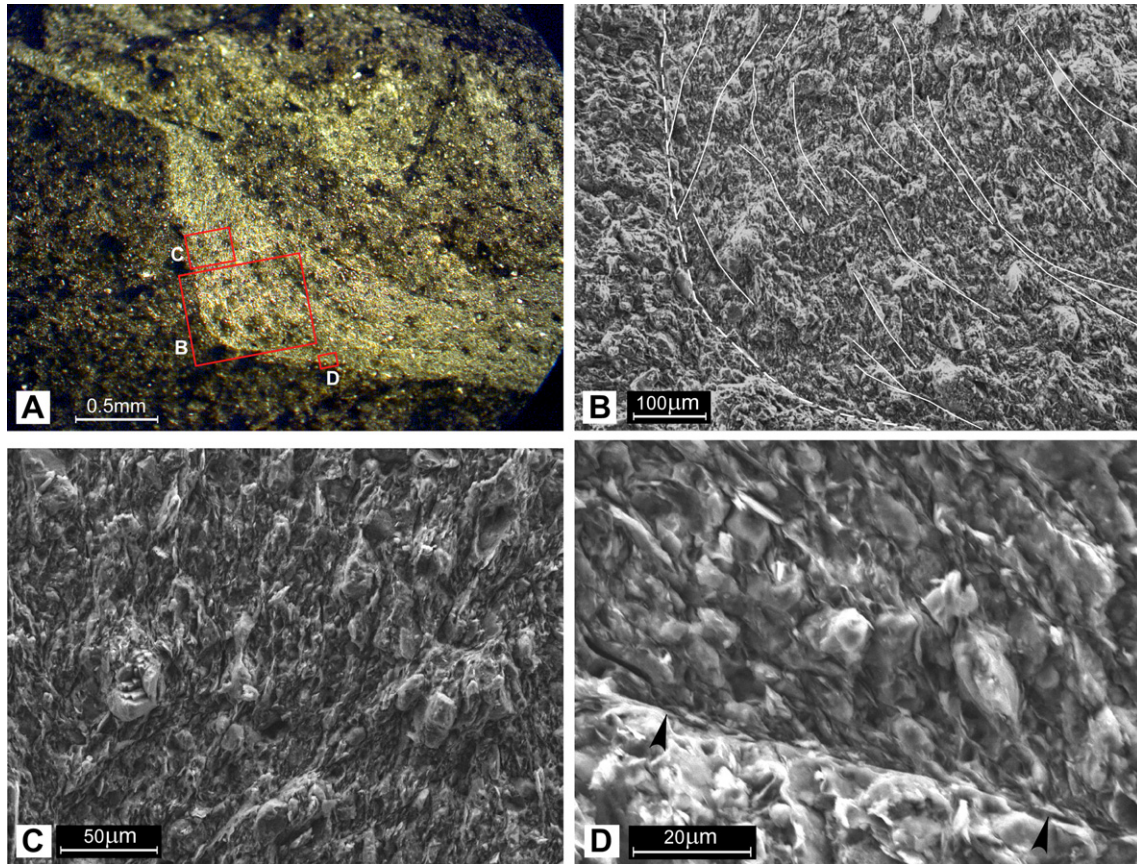
**Fig. 13.** A - Microphotograph of the step-like asperity along a shear filled with illitic mudstone in sample T3 (Fig. 12). The location of secondary electron SEM images is indicated by rectangles. B − Low-magnification SEM image of the boundary (dashed line) between smectitic and illitic mudstone. The illitic filling of the shear presents a fabric marked by particles elongation and microshears (white lines) that gradually curves with the shear boundary. C - Enlargement of the fabric within the illitic infill of the shear. D - The boundary of the shear (arrows) is very sharp and within the illitic fill particles are aligned to form angles of 140°−150° with the shear direction.

sediments (Mitchell and Soga, 2005; Nygård et al., 2006). The overconsolidation ratio is expressed as:

$$OCR = P_{effmax}/P_{effcurr}$$

where $P_{effmax}$ is the maximum vertical effective stress experienced by sediments and $P_{effcurr}$ is the present vertical effective stress. Materials that have never sustained effective stresses larger than the current one are termed normally consolidated (NC), whereas sediments that in the past experienced greater effective vertical stresses are termed overconsolidated (OC). If present, this larger effective stress recorded by a mudstone is known as a pre-consolidation stress. Overconsolidation has an important effect on the compressibility and shear behaviour of mudstones. During compression (consolidation), OC mudstones are much stiffer than NC mudstones and the compression curve, expressed in terms of volumetric strain vs. effective stress, of OC mudstones is much flatter than NC ones (Crawford, 1986; Nygård et al., 2006). It is thus possible to determine the pre-consolidation (yield) stress from the shape of the compression curve, which changes its slope once the pre-consolidation stress is exceeded (post-yield domain).

An intact sample of mudstone extracted from the fault's footwall was carefully trimmed and placed in the oedometer ring. The unsaturated sample was soaked in de-ionised water under a constant vertical stress (2 MPa) to avoid any important destructuration on wetting (swelling strain under these conditions was limited to 1%). The sample was then loaded and unloaded under saturated conditions following a stepwise procedure. Each loading

step increment (3 MPa) was maintained for three days to allow for the dissipation of pore pressure. The compression curve of the mudstones forming the footwall of the shear zone shows swelling under load (2 MPa), as path AB, and loading/unloading as path BCD (Fig. 16). The test was conducted on the footwall mudstones because these are expected to have experienced deeper burial than the hangingwall. Two procedures were followed to determine the preconsolidation stress, namely the change in the maximum curvature zone between the pre-yield and the post-yield compressibility domains, and the zone undergoing significant changes in the cumulative work input per unit volume on loading (i.e., the zone in which the slope of the curve -cumulative work input versus log vertical effective stress- displays a sudden change) (Romero, 1999). Both procedures yield a pre-consolidation stress of approximately 10 MPa (Fig. 16).

In the absence of any fluid pressure, the vertical stress ($\sigma_v$) generated by an overburden is given by:

$$\sigma_v = \rho g z \tag{1}$$

where $\rho$ is the bulk density of the sedimentary column, $g$ is the acceleration due to gravity and $z$ the depth. Given a $\sigma_v$ of 10 MPa and Eq. (1) in the form:

$$z = \sigma_v/(\rho g), \tag{2}$$

the burial depth can be determined if density is known. The bulk density of 2 samples collected from the fault footwall were measured using a helium pycnometer (Multivolume Pycnometer
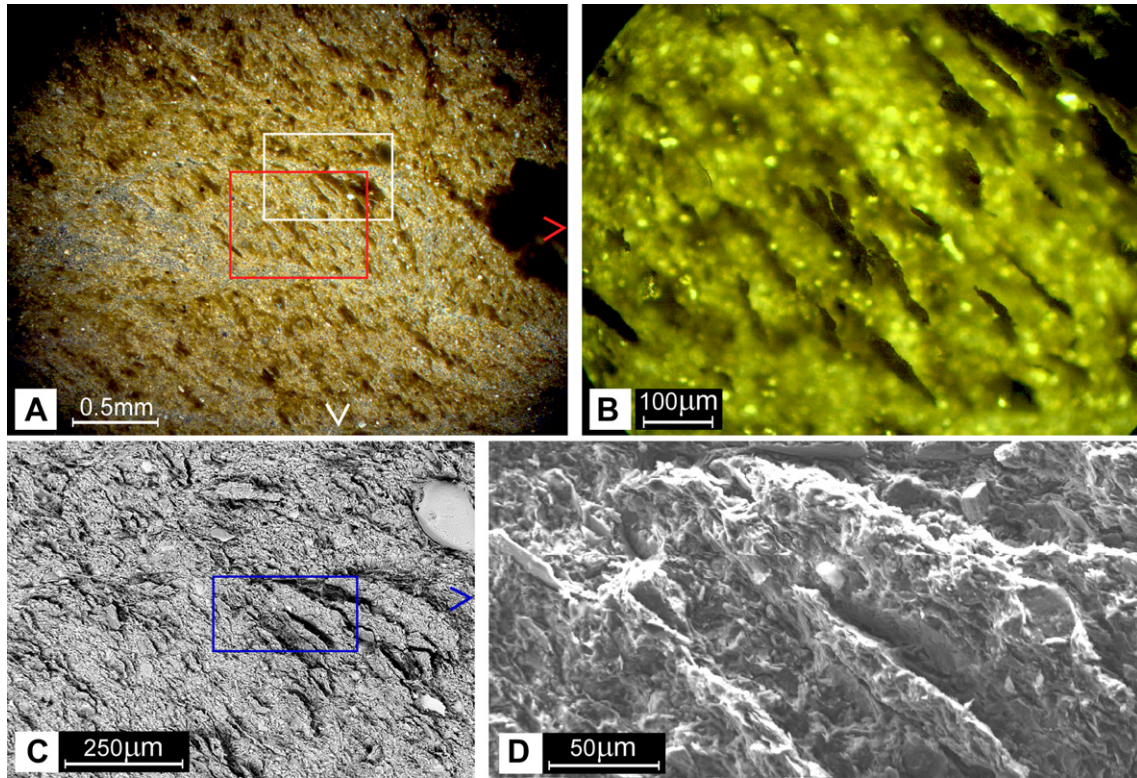
**Fig. 14.** A - Crossed Nicols microphotograph of a small area of peel T3 along an illitic veinlet, location in Fig. 12. B - Enlargement of the area marked by box in A. Large platy features, of supposedly smectitic composition, are oriented parallel to the P foliation and protrude out of the peel's surface. C - Backscattered electron image of the area marked by white box in A. D - SEM image of boxed area in C.
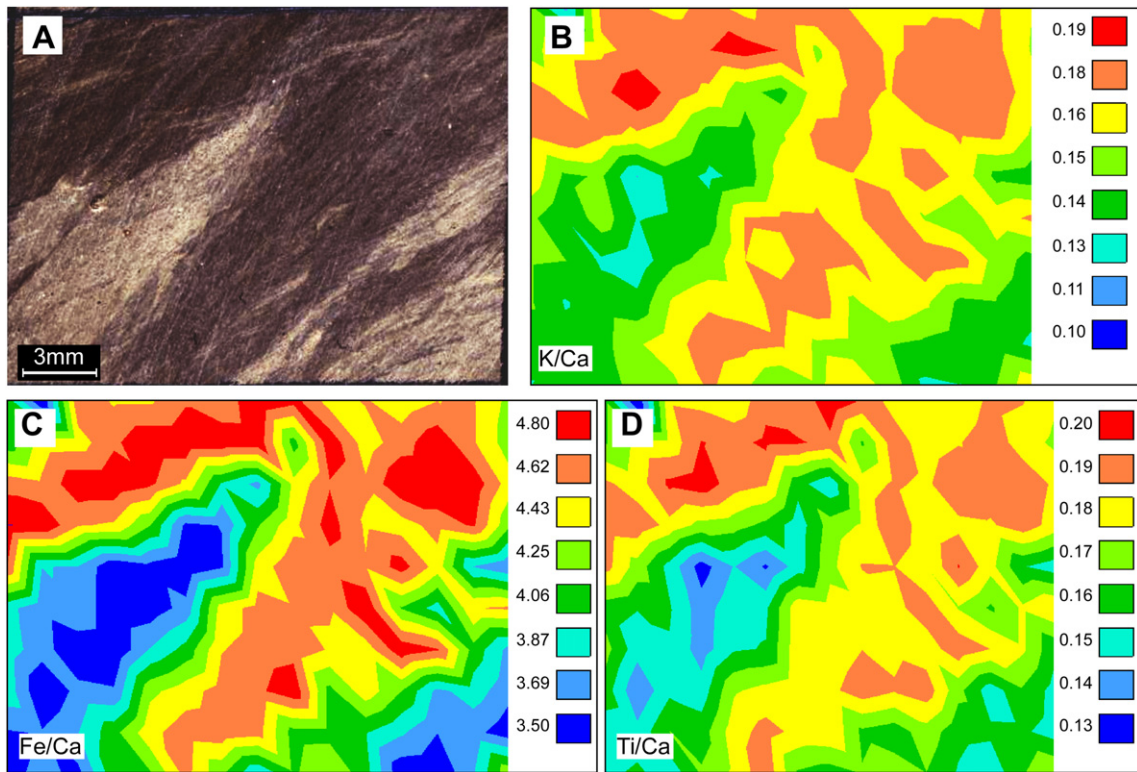


**Fig. 15.** Results of X-ray fluorescence mapping on the small area of sample T2 shown in A. B - Distribution pattern of K with respect to Ca, indicating that the dark-coloured illitic mudstone is enriched in K. C - The distribution pattern of Fe shows a large gradient between the Fe-rich illite and Ca-rich smectite. D - Map distribution of the Ti/Ca ratio indicating that the illitic component is enriched in Ti.
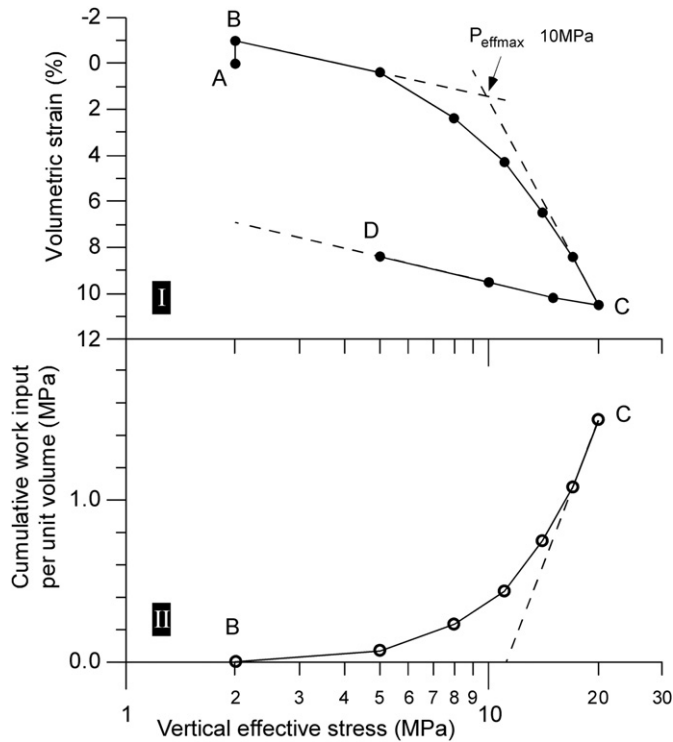
**Fig. 16.** Consolidation curve (I) and evolution of the cumulative work input per unit volume (II) of the mudstone composing the footwall of the studied shear zone. A–B in the upper diagram is the saturation-related swelling. B–C and C–D are the loading and unloading paths, respectively, with work input for loading shown in II. The calculated pre-consolidation stress is about 10 MPa.

1305, Micromeritcs®). An average value of 2.7 g/cm$^3$ was obtained. Using this measured density in Eq. (2) yields a burial depth of 378 m. In the presence of a fluid pressure (P), effective rather than lithostatic stresses should be used and $\sigma_v$ in Eq. (1) & (2) would be replaced by $(\sigma_v - P)$. Thus, if fluid pressure was present, the rock was buried deeper than 378 m.

## 7. Discussion

### 7.1. Textural observations

Peels show that, along the P foliation (i.e., a flattening fabric, Fig. 6A), domains of mixed layer smectite-illite and illite coexist on a sub-millimetre scale (Fig. 10 and Fig. 11A). The P foliation is a salient characteristic of the shear zone, highlighted by the preferred orientation of mud cracks (Fig. 5) and platy particles (Fig. 14). The re-orientation of platy particles can be achieved through their mechanical rotation or through processes of dissolution and re-crystallization (Knipe, 1981; Price and Cosgrove, 1990). This latter process is considered by previous workers (Buatier et al., 1992; Yan et al., 2001; Stixrude and Peacor, 2002; Charpentier, 2003) to be the primary mechanism for the transformation of smectite into illite. On the basis of their identical orientation and process of formation, we propose that the P foliation and the observed illitic domains formed at the same time. During this transformation interlayer water from the smectite is released and illite, which is characterized by higher density and smaller volume, is formed (Yan et al., 2001; Mondol and Johron, 2008).

If the smectite to illite transformation was a result of the overall temperature in the basin it would not be restricted to the shear zone. Nevertheless, it might be argued that the temperature within the zone was increased by fictional heating (e.g. Hirono et al., 2008; Kuo et al., 2011; Hamada et al., 2011) or by warm fluid pulses. However, the P foliation is a flattening fabric along which negligible shear and fluid flow is thought to occur. Therefore, it seems unlikely that illitization was a result of heating caused by friction or by warm fluids transported along shears.

Shears filled with illitic mudstone (Fig. 12) indicate that illitization also occurs along shear planes. These shear planes are mostly oriented as P shears, forming an angle ∼165° with the shear zone boundary (Fig. 6A and Fig. 12) and, unlike Y shears they are not suitably oriented to sustain the large displacements (i.e. metres scale) that are necessary to develop high temperatures. The illitic infill of these shears is characterised by a strong fabric, marked by the preferred orientation of elongate particles, abundant microshears (Fig. 13B–C), and by smectitic fragments transported within the shears. We argue that the localization of shear strain within these zones enhances the breakdown of smectite to illite and the associated release of water. It should be noted in this regard that the presence of untransformed smectite within the illitic fillings of shears (Figs. 4, 10 and 12) represents a potential source of water inside the shear zone. Progressive dehydration of this smectite would then release water and further lubricate the zone.

### 7.2. Conditions of formation

When discussing the transformation of smectite into illite, a crucial point is the identification of the physical and/or chemical conditions that triggered the reaction. Currently temperature and the availability of K$^+$ ions are considered to be the primary factors governing this diagenetic transformation (Hower et al., 1976; Huang et al., 1993; Cuadros, 2006). Secondary factors are time, rock/water ratio, fluid and rock composition, and pressure (Colten-Bradley, 1987; Whitney, 1990; Drief et al., 2002).

However, because the studied shear zone was uplifted and eroded during the Pleistocene, and since it lacks mineralised veins, it is extremely difficult to evaluate the relative importance of these factors. The geological setting of the Sant'Arcangelo basin, which is composed largely of clastic units originating from the erosion of igneous rocks containing K-feldspars and mica (Carbone et al., 1991), suggests that K$^+$ ions were available in the circulating fluids. Some authors have suggested that fluids rich in ions induce illitization within shears and faults (e.g. Abid and Hesse, 2007; Dellisanti et al., 2008). However, as discussed in the previous Section (7.1), the observed patterns of illitization along planes of flattening suggest that fluid chemistry is not the primary factor causing the mineral transformation.

Defining the temperature at which illitization occurred is a difficult task. A tool frequently used to determine the diagenetic stage of buried sediments is the measure of illite crystallinity (Kübler index; Kübler and Jaboyedoff, 2000; Essene and Peacor, 1995). Unfortunately, this approach cannot be used for the illite contained in the mudstones of the Sant'Arcangelo basin because they are predominantly detrital in origin and would therefore provide information on the original rock suite rather than the diagenetic conditions inside the basin (e.g. Dellisanti et al., 2008). The consolidation test performed on the footwall mudstones (Fig. 16) provides an approximate measure of the maximum effective vertical stress experienced by the wallrock sediments (10 MPa), which, in the absence of any fluid pressure, corresponds to a very shallow burial depth (∼378 m below sea floor). Because the magnitude of any fluid pressure in the rock is unknown, the actual depth of burial, and consequently the maximum temperature at which the shear zone formed, cannot be determined. However, an indication regarding the amount of uplift and erosion experienced by the sediments of this basin comes from

geomorphologic studies of the uplifted marine and fluvial terraces. These studies indicate that since 3.1 Ma (Late Pliocene) the region was uplifted ~1370 m (Westaway and Bridgland, 2007). These data, suggest that the diagenetic conditions of the studied mudstones at the time of formation of the shear zone were milder (depth probably < 2 km; $T < 60\ °C$) than is generally accepted to be necessary for smectite to transform in illite (i.e. depths 1–5 km; temperature $70°$–$160\ °C$, see e.g. Bruce, 1984; Pollastro, 1985; Cuadros, 2006).

Finally, it is important to remark that whatever the P-T conditions in the mudstones of the Sant'Arcangelo basin were during the transformation, illitization occurred exclusively inside the shear zone and the illite formed along planar domains parallel to the P foliation (Fig. 10 and Fig. 11A). These observations indicate clearly the link between shear deformation and the process of illitization.

## 8. Summary

The present study documents the transformation of smectite into illite in a large strike-slip fault zone. This mineral transformation leads to a darkening in colour of the mudstone. The heterogeneous distribution of smectitic and illitic domains within the fault was analyzed employing a peeling technique using a fastening agent that adheres to mudstones according to their properties (i.e. porosity, mineralogy etc.) and that produces peels that can be studied with microscope and SEM. Smectite disappearance due to replacement by illite occurs in planar domains elongated parallel to the P foliation. Illite also occurs along the shears. The ductile geometries in the illite along the shears and the evidence of multiple events of shearing suggest that these shears acted as channels for the water released by smectite dehydration. The geological framework and the consolidation characteristics of the relatively undeformed rocks in the shear zone walls suggest that the fault deformed under P-T conditions that are too low to initiate the smectite/illite transformation. These observations, together with reports of similar illite enrichment in other fault gouges, highlight the need for a re-evaluation of the factors that stimulate smectite illitization within faults. The present authors argue that the illitization processes observed in the Scorciabuoi shear zone provide a mechanism for the local generation of high fluid pressures which can considerably facilitate fault movement. More generally it is argued that the process of stress-induced illitization of smectite that occurs in fault zones, may generate fluid overpressure with consequent mechanical weakening that occurs at plate boundary subduction thrusts (e.g. Tobin and Saffer, 2009).

## Acknowledgements

## Appendix. Supplementary material

Supplementary data associated with this article can be found, in the online version, at doi:10.1016/j.jsg.2011.08.002.

## References

Abid, I., Hesse, R., 2007. Illitizing fluids as precursors of hydrocarbon migration along transfer and boundary fault of the Jeanne d'Arc Basin offshore Newfoundland, Canada. Marine and Petroleum Geology 24, 237–245.

Arch, J., Maltman, A., 1990. Anisotropic permeability and tortuosity in deformed wet sediments. Journal of Geophysical Research 95, 9035–9045.

Bailey, W.R., Underschultz, J., Dewhurst, N.N., Kovack, G., Mildren, S., Raven, S., 2006. Multi-disciplinary approach to fault and top seal appraisal; Pyrenees−Macedon oil and gas fields, Exmouth Sub-basin, Australian Northwest Shelf. Marine and Petroleum Geology 23, 241–259.

Bangs, N.L., Shipley, T.H., Moore, J.C., Moore, G.F., 1999. Fluid accumulation and channelling along the Northern Barbados Ridge décollement thrust. Journal of Geophysical Research 104, 20399–20414.

Benvenuti, M., Bonini, M., Moratti, G., Sani, F., 2006. Tectonosedimentary evolution of the Plio-Pleistocene Sant'Arcangelo basin (southern Apennines, Italy). In: Moratti, G., Chalouan, A. (Eds.), Tectonics of the Western Mediterranean and North Africa. Geological Society, London, Special Publication, vol. 262, pp. 289–322.

Bonini, M., Sani, F., 2000. Pliocene-Quaternary transpressional evolution of the Anzi-Calvello and northern S. Arcangelo basins (Basilicata, southern Apennines, Italy) as a consequence of deep-seated fault reactivation. Marine and Petroleum Geology 17, 909–927.

Bos, B., Spiers, C.J., 2001. Experimental investigation into the microstructural and mechanical evolution of phyllosilicate-bearing fault rock under conditions favouring pressure solution. Journal of Structural Geology 23, 1187–1202.

Boyer, S.E., Elliot, D., 1982. Thrust systems. AAPG Bulletin 66, 1196–1230.

Brown, R.J., 1986. SEM examination of carbonate microfacies using acetate peels. Journal of Sedimentary Research 56 (4), 538–543.

Brown, K.M., Saffer, D.M., Bekins, B.A., 2001. Smectite diagenesis, pore-water freshening, and fluid flow at the toe of the Nankai wedge. Earth and Planetary Science Letters 194, 97–109.

Brown, K.M., Kopf, A., Underwood, M., Weinberger, J., 2003. Compositional and fluid pressure controls on the state of stress on the Nankai subduction thrust: a weak plate boundary. Earth and Planetary Science Letters 214, 589–603. doi:10.1016/S0012-821X(03)00388-1.

Bruce, C.H., 1984. Smectite dehydration-its relation to structural development and hydrocarbon accumulation in Nothern Gulf of Mexico basin. AAPG Bulletin 68, 673–683.

Buatier, M.D., Peacor, D.R., O'Neil, J., 1992. Smectite illite transition in Barbados accretionary wedge sediments: TEM and AEM evidence for dissolution Cristallization at low temperature. Clays and Clay Minerals 40, 65–80.

Capuano, R.M., 1993. Evidence of fluid flow in microfractures in geopressured shales. AAPG Bullettin 77, 1303–1314.

Caputo, R., Salviulo, L., Bianca, M., 2008. Late quaternary activity of the Scorciabuoi Fault (Southern Italy) as inferred from morphotectonic investigations and numerical modeling. Tectonics 27, TC3004. doi:10.1029/2007TC002203.

Carbone, S., Catalano, S., Lazzari, S., Lentini, F., Monaco, C., 1991. Presentazione della Carta Geologica del bacino del Fiume Agri (Basilicata). Memorie Società Geologica Italiana 47, 129–143.

Casciello, E., Cesarano, M., Cosgrove, J.W., 2004. Shear deformation of pelitic rocks in a large-scale natural fault. In: Alsop, G.I., Holdsworth, R.E., McCaffrey, K.J.W., Hand, M. (Eds.), Flow Processes in Faults and Shear Zones. Geological Society, London, Special Publication, vol. 224, pp. 113–125.

Catalano, S., Monaco, C., Tortorici, L., Paltrinieri, W., Steel, N., 2004. Neogene-quaternary evolution of the Southern Apennines. Tectonics 23. doi:10.1029/2003TC001512.

Charpentier, D., 2003. Fabric development and the smectite to illite transition in Gulf of Mexico mudstones: an image analysis approach. Journal of Geochemical Exploration 78–79, 459–463.

Colten-Bradley, V.A., 1987. Role of pressure in smectite dehydration- effects on geopressure and smectite-to-illite transformation. AAPG Bulletin 71, 1414–1427.

Crawford, C.B., 1986. State of the art: evaluation and interpretation of soil consolidation tests. In: Yong, R.N., Townsend, F.C. (Eds.), Consolidation of Soils: Testing and Evaluation, pp. 71–103. ASTM STP 892, Philadelphia.

Cuadros, J., 2006. Modeling of smectite illitization in burial diagenesis environments. Geochimica et Cosmochimica Acta 70, 4181–4195.

Dellisanti, F., Pini, G.A., Tateo, F., Baudin, F., 2008. The role of tectonic shear strain on the illitization mechanism of mixed-layers illite-smectite. A case study from a fault zone in the Northern Apennines, Italy. International Journal of Earth Sciences 97, 601–616.

Dewhurst, D.N., Brown, K.M., Clennell, M.B., Westbrook, G.K., 1996. A comparison of the fabric and permeability anisotropy of consolidated and sheared silty clay. Engineering Geology 42, 253–267.

Dewhurst, D.N., Hennig, A.L., 2003. Geomechanical properties related to top seal leakage in the Carnarvon Basin, Northwest Shelf, Australia. Petroleum Geoscience 9, 255–263.

Drief, A., Martinez-Ruiz, F., Nieto, F., Velilla Sanchez, N., 2002. Transmission electron microscopy evidence for experimental illitization of smectite in K-enriched seawater solution at 50°C and basic pH. Clays and Clay Minerals 50 (6), 746–756.

Essene, E.J., Peacor, D.R., 1995. Clay mineral thermometry - a critical perspective. Clays and Clay Minerals 43, 540–553.

Faulkner, D.R., Rutter, E.H., 2001. Can the maintenance of overpressured fluids in large strike-slip fault zones explain their apparent weakness? Geology 29, 503–506.

Fitts, T.G., Brown, K.M., 1999. Stress-induced smectite dehydration: ramifications for patterns of freshening and fluid expulsion in the N Barbados accretionary wedge. Earth and Planetary Science Letters 172, 179–197.

Haines, S.H., Van der Pluijm, B.A., Ikari, M.J., Saffer, D.M., Marone, C., 2009. Clay fabric intensity in natural and artificial fault gouges: implications for brittle fault zone processes and sedimentary basin clay fabric evolution. Journal of Geophysical Research 114, B05406. doi:10.1029/2008JB005866.

Hamada, Y., Hirono, T., Ishikawa, T., 2011. Coseismic frictional heating and fluid-rock interaction in a slip zone within a shallow accretionary prism and implications for earthquake slip behaviour. Journal of Geophysical Research 116, B01302. doi:10.1029/2010JB007730.

Henry, P., Bourlange, S., 2004. Smectite and fluid budget at Nakai OPD sites derived from cation exchange capacity. Earth and Planetary Science Letters 219, 129–145.

Hippolyte, J.C., Angelier, J., Roure, F., Casero, P., 1994a. Piggyback development and thrust belt evolution: structural and paleostress analysis of Plio-Quaternary basin in the Southern Apennines. Journal of Structural Geology 16, 159–173.

Hippolyte, J.C., Angelier, J., Roure, F., 1994b. A major geodynamic change revealed by quaternary stress patterns in the Southern Apennines (Italy). Tectonophysics 230, 199–210.

Hirono, T., Fujimoto, K., Yokoyama, T., Hamada, Y., Tanikawa, W., Tadai, O., Mishima, T., Tanimizu, M., Lin, W., Soh, W., Song, S.-R., 2008. Clay mineralogy reactions caused by frictional heating during an earthquake: an example from the Taiwan Chelungpu fault. Geophysical Research Letters 35, L16303. doi:10.1029/2008GL034476.

Hower, J., Eslinger, E., Hower, M.E., Perry, E.A., 1976. Mechanism of burial and metamorphism of argillaceous sediment: 1 mineralogical and chemical evidence. Geological Society of America Bulletin 87, 725–737.

Huang, W.H., Longo, J.M., Pevear, D.R., 1993. An experimental derived kinetic model for the smectite-to-illite conversion and its use as a geothermometer. Clays Clay Miner 41, 162–177.

Ikari, M.J., Saffer, D.M., Marone, C., 2009. Frictional and hydrologic properties of clay-rich fault gouge. Journal of Geophysical Research 114, B05409. doi:10.1029/2008JB006089.

Ingram, G.M., Urai, J.L., 1999. Top-seal leakage through faults and fractures: the role of mudrock properties. In: Aplin, A., Fleet, A.J., Macquaker, J.H.S. (Eds.), Muds and Mudstones: Physical and Fluid Flow Properties. Geological Society, London, Special Publication, vol. 158, pp. 125–135.

Knipe, R.J., 1981. The interaction of deformation and metamorphism in slates. Tectonophysics 78, 249–272.

Kübler, B., Jaboyedoff, M., 2000. Illite crystallinity. In: Comptes Rendus de l'Académie des Sciences - Series IIA - Earth and Planetary Science, vol. 331(2), pp. 75–89.

Kuo, L.-W., Song, S.-R., Huang, L., Yeh, E.-C., Chen, H.-F., 2011. Temperature estimates of coseismic heating in clay-rich fault gouges, the Chelungpu fault zones, Taiwan. Tectonophysics 502, 315–327.

Logan, J.M., Dengo, C.A., Higgs, N.G., Wang, Z.Z., 1992. Fabrics of experimental fault zones: their development and relationship to mechanical behaviour. In: Evans, B., Wong, T. (Eds.), Fault Mechanics and Transport Properties of Rocks. Academic Press, London, pp. 33–67.

Maggi, C., Frepoli, A., Cimini, G.B., Console, R., Chiappini, M., 2008. Recent seismicity and crustal stress field in the Lucanian Apennines and surrounding areas (Southern Italy): seismotectonic implications. Tectonophysics 463, 130–144.

Maltman, A.J., 1987. Shear zones in argillaceous sediments - an experimental study. In: Jones, M.E., Preston, R.M.E. (Eds.), Deformation of Sedimentary Rocks. Geological Society, London, Special Publication, vol. 29, pp. 77–87.

Maltman, A.J., Vannucchi, P., 2004. Insights from the Ocean Drilling Program on shear and fluid-flow at the mega-faults between actively converging plates. In: Alsop, G.I., Holdsworth, R.E., McCaffrey, K.J.W., Hand, M. (Eds.), Flow Processes in Faults and Shear Zones. Geological Society, London, Special Publication, vol. 224, pp. 127–140.

Merriman, R.J., Peacor, D.R., 1999. Very low-grade metapelites: mineralogy, microfabrics and measuring reaction progress. In: Frey, M., Robinson, D. (Eds.), Low-grade Metamorphism. Blackwell Science, p. 313.

Mitchell, J.K., Soga, K., 2005. Fundamentals of Soil Behaviour. John Wiley & Sons, New Jersey.

Monaco, C., Tortorici, L., Paltrinieri, W., 1998. Structural evolution of the Lucanian Appennines, Southern Italy. Journal of Structural Geology 20 (5), 617–638.

Monaco, C., Tortorici, L., Catalano, S., Paltrinieri, W., Steel, N., 2001. The role of Pleistocene strike-slip tectonics in the Neogene-Quaternary evolution of the Southern Apennine orogenic belt: implications for oil trap development. Journal of Petroleum Geology 24 (3), 339–359.

Mondol, N.H., Jahren, J., 2008. Elastic properties of clay minerals. The Leading Edge 27, 758–770.

Moore, D.E., Summers, R., Byerlee, J.D., 1989. Sliding behaviour and deformation textures of heated illite gouge. Journal of Structural Geology 11, 329–342.

Moore, J.C., Saffer, D., 2001. Updip limit of the seismogenic zone beneath the accretionary prism of southwest Japan: an effect of diagenetic to low-grade metamorphic processes and increasing effective stress. Geology 29, 183–186.

Nygård, R., Gutierrez, M., Bratli, R.K., Høeg, K., 2006. Brittle-ductile transition, shear failure and leakage in shales and mudrocks. Marine and Petroleum Geology 23, 201–212.

Pieri, P., Sabato, L., Loiacono, F., Marino, M., 1994. Il bacino di piggy back di Sant'Arcangelo: evoluzione tettonico-sedimentaria. Bollettino Società Geologica Italiana 113, 465–481.

Pieri, P., et al., 1997. Tettonica Quaternaria nell'area Bradanico-Ionica. Il Quaternario 10 (2), 535–542.

Pollastro, R.M., 1985. Mineralogical and morphological evidence for the formation of illite at the expense of illite/smectite. Clays and Clay Minerals 33, 265–274.

Price, N., Cosgrove, J.W., 1990. The Analysis of Geological Structures. Cambridge University Press, Cambridge.

Romero, E., 1999. Characterisation and thermo-hydro-mechanical behaviour of unsaturated Boom clay: an experimental study, PhD Thesis, Universitat Politecnica de Catalunya, http://www.tdx.cat/TDX-0930102-092135.

Rutter, E.H., Maddock, R.H., Hall, S.H., White, S.H., 1986. Comparative microstructures of natural and experimentally produced clay-bearing gouges. Pure and Applied Geophysics 124, 3–29.

Saffer, D.M., Bekins, B.A., 1998. Episodic fluid flowin the Nankai accretionary complex: timescale, geochemistry, flow rates and fluid budget. Journal of Geophysical Research 103 (B12), 30351–30370.

Saffer, D.M., Marone, C., 2003. Comparison of smectite and illite-rich gouge frictional properties: application to the updidp limit of the seismogenic zone along subduction megathrusts. Earth and Planetary Science Letters 215, 219–235.

Saffer, D.M., Bekins, B.A., 2006. An evaluation of factors influencing pore pressure in accretionary complexes: implications for taper angle and wedge mechanics. Journal of Geophysical Research 111, B04101. doi:10.1029/2005JB003990.

Shipley, T.H., Moore, G.E., Bangs, N.L., Moore, J.C., Stoffa, E.L., 1994. Seismically inferred dilatancy distribution, Northern Barbados Ridge décollement - implications for fluid migration and fault strength. Geology 22, 411–414.

Solum, J., van der Pluijm, B.A., Peacor, D., 2005. Neocrystallization, fabrics and age of clay minerals from an exposure of the Moab Fault, Utah. Journal of Structural Geology 27, 1563–1576. doi:10.1016/j.jsg.2005.05.002.

Solum, J.G., van der Pluijm, B.A., 2009. Quantification of fabrics in clay gouge from the Carboneras fault, Spain, and implications for fault behaviour. Tectonophysics 475 (3–4), 554–562. doi:10.1016/j.tecto.2009.07.006.

Stixrude, L., Peacor, D.R., 2002. First-principles study of illite – smectite and implications for clay mineral systems. Nature 420, 165–168.

Takizawa, S., Kamai, T., Matsukura, Y., 2005. Fluid pathways in the shearing zones of kaolin subjected to direct shear tests. Engineering Geology 78, 135–142.

Tobin, H.J., Saffer, D.M., 2009. Elevated fluid pressure and extreme mechanical weakness of a plate boundary thrust, Nankai trough subduction zone. Geology 37 (8), 679–682.

Ujiie, K., Tsutsumi, A., Fialko, Y., Yamaguchi, H., 2009. Experimental investigation of frictional melting of argillite at high slip rates: implications for seismic slip in subduction-accretion complexes. Journal of Geophysical Research 114, B04308. doi:10.1029/2008JB006165.

Vrolijk, P.J., van der Pluijm, B.A., 1999. Clay gouge. Journal of Structural Geology 21, 1039–1048. doi:10.1016/S0191-8141(99)00103-0.

Weaver, C.F., 1960. Possible uses of clay minerals in search for oil. AAPG Bulletin 44 (9), 1505–1518.

Westaway, R., Bridgland, D., 2007. Late Cenozoic uplift of southern Italy deduced from fluvial and marine sediments: coupling between surface processes and lower-crustal flow. Quaternary International 175, 86–124.

Whitney, C., 1990. Role of water in the smectite-to-illite reaction. Clay and Clay Minerals 38, 343–350.

Woodcock, N.H., Fischer, M., 1986. Strike-slip duplexes. Journal of Structural Geology 8, 737–752.

Yan, Y., van der Pluijm, B., Peacor, D., 2001. Deformational microfabrics of clay gouge, Lewis Thrust, Canada: a case for fault weakening from clay transformation. In: Holdsworth, R.E., Strachan, R.A., Magloughlin, J.F., Knipe, R.J. (Eds.), The Nature and Tectonic Significance of Fault Zone Weakening. Geological Society, London, Special Publication, vol. 186, pp. 103–112.

Zeng, J., Yu, C., 2006. Hydrocarbon migration along the Shengbei fault zone in the Bohai Bay basin, China: the evidence from geochemistry and fluid inclusions. Journal of Geochemical Exploration 89, 455–459.

Zhang, S., Cox, S., 2000. Enhancement of fluid permeability during shear deformation of a synthetic mud. Journal of Structural Geology 22, 1385–1393. doi:10.1016/S0191-8141(00)00065-1.